CORRELATIONS BETWEEN SCAL PARAMETERS AND POROSITY/PERMEABILITY: A COMPARISON BETWEEN EXPERIMENTAL DATA AND SIMULATED DATA FROM A PORE NETWORK SIMULATOR

A.W. Cense[1], R. Miskiewicz[2], R.M.M. Smits[1], X.D. Jing[1]
[1]Shell International, Kessler Park 1, 2288 GS, Rijswijk, The Netherlands [2]Delft University of Technology, P.O. Box 5, 2600 AA, Delft, The Netherlands

This paper was prepared for presentation at the International Symposium of the Society of Core Analysts held in Halifax, Nova Scotia, Canada, 4-7 October, 2010

ABSTRACT

In this paper, we compare simulated data from a pore network simulator with experimental data in a much more general way than has been reported in literature so far. For a large number of sandstone fields, we have measured capillary pressure and relative permeability during drainage and imbibition conditions. The experimental data was fitted with the aid of the Brooks-Corey (drainage capillary pressure), Skjaeveland (primary imbibition capillary pressure) and Corey (relative permeability) correlations. Subsequently, correlations between the parameters that describe these curves and the permeability and porosity of the complete set of samples were established. The same procedure was repeated for a data set of virtual rock samples. These rocks were obtained by a process-based reconstruction technique on the basis of grain size distributions for Bentheimer, Berea and Fontainebleau sandstones and a sandstone reservoir rock. The rock models were given a range of porosities, permeabilities and wettabilities that covered the experimental data set. Relative permeability and capillary pressure were obtained from flow simulations on the pore network model of each virtual rock. Fitting parameters, plotted against permeability and porosity, resulted in a second set of correlations. Both sets of data were compared. It was found that trends in drainage capillary pressure parameters agreed well. Simulated imbibition-relative permeability parameters showed an inconsistent wettability trend in the water Corey exponent. Trends in wettability indices for simulations on mixed-wet-small, mixed-wet-large and fractionally-wet models were not in agreement with previous findings from literature.

INTRODUCTION

Since the first introduction of pore network models by Fatt (Fatt, 1956), the predictive power of pore network models has increased. Whereas comparative studies were initially focused on outcrop material (Berea, Fontainebleau, Bentheimer (Bakke and Øren, 1997; Øren *et al.*, 1997)), considerable work has been done in the last decade to make comparisons for reservoir rocks (Caubit *et al.*, 2008, Øren *et al.*, 2006).

In the workflow of pore network modelling a 3D model of the rock is required, which is obtained via micro CT scanning (see *e.g.* Sakellariou *et al.*, 2004), process based modelling (Bakke *et al.*, 1997) or multi-point statistical methods (Quiblier, 1984). Calculations of porosity, permeability and nowadays also primary drainage capillary pressure can be performed directly on the 3D image. To calculate the imbibition capillary pressure, relative permeabilities and resistivity index, a simplification step is needed: the 3D image is converted to a representative pore network model (in this study, primary drainage capillary pressure was obtained from simulations on the pore network model).

Most of the comparative studies hitherto published in open literature provide direct comparisons between simulated data and experimental data for specific outcrop or reservoir rock material. In many cases, good matches are found for the porosity, permeability and primary drainage of (sandstone) outcrop materials (*e.g.* Bakke *et al.* (1997), Øren *et al.* (2002)). Since wettability cannot be predicted, the results for imbibition capillary pressure and relative permeability are matched by tuning the contact angles and by changing the fraction of oil wet pores. However, since capillary pressure and relative permeability are coupled parameters, a match of the (imbibition) capillary pressure does not always guarantee a match of the (imbibition) relative permeability. Comprehensive studies, where porosity, permeability, drainage and imbibition properties are compared against experimental data, are scarce. The limitations of the comparative studies done so far are such that it is difficult to generalize results. What works for one reservoir might not be valid for the other.

In this study, an alternative approach is chosen to validate pore network modelling results with experimental data. We do not make a direct comparison on specific samples. Instead, we compare an experimental dataset, generated in-house, and a virtual dataset that was generated with the aid of pore network modelling software on the basis of high-level correlations between SCAL parameters (*e.g.* entry pressure, irreducible water saturation, Corey exponents) and porosity, permeability and wettability.

MATERIALS AND METHODS

Experimental database

Capillary pressure measurements were performed in-house on 443 sandstone samples from various fields. Experiments included primary drainage, primary imbibition and secondary drainage. USBM and Amott-Harvey wettability indices were determined. The USBM index (Donaldson *et al.*, 1969) was calculated from centrifuge data, without using a capillary pressure cut-off. Where possible, results were interpreted with Shell's reservoir simulator MoReS, to correct for capillary end effects. Primary drainage capillary pressure data was fitted with the Brooks-Corey equation (Brooks and Corey, 1964):

$$P_c^{\,d} = \frac{P_e}{\left[\dfrac{S_w - S_{ir}}{1 - S_{ir}}\right]^a}, \qquad (1)$$

where P_c is the capillary pressure, P_e is the entry pressure, S_w is the water saturation, S_{ir} is the irreducible water saturation and a is a curve shape factor. Primary imbibition data was matched using the (modified) Skjaeveland description (Skjaeveland *et al.* (2000)):

$$P_c^{\,i} = \frac{c_w}{\left[\frac{S_w - S_{ir}}{1 - S_{ir}}\right]^{a_w}} - \frac{c_o}{\left[\frac{1 - S_w - S_{or}}{1 - S_{or}}\right]^{a_o}}, \tag{2}$$

where c_w and c_o are 'entry pressure' coefficients, a_w and a_o are curve shape parameters and S_{or} is the residual oil saturation. We modified the original equation by changing the plus sign in the original equation to a minus sign, so that all coefficients are positive.

Relative permeability measurements were performed on 74 samples from 13 sandstone reservoirs, using steady state or centrifuge techniques. Where required, results were interpreted with the aid of a reservoir simulator (MoReS). All imbibition relative permeability data was fitted by means of the Corey representation:

$$k_{rw} = k_{rw}(S_{or})\left[\frac{S_w - S_{ir}}{1 - S_{ir} - S_{or}}\right]^{n_w}, \tag{3}$$

$$k_{ro} = k_{ro}(S_{ir})\left[\frac{1 - S_w - S_{or}}{1 - S_{ir} - S_{or}}\right]^{n_o}, \tag{4}$$

For each parameter in Eq. (1) to (4) correlations were established with $X = \sqrt{\frac{k}{\varphi}}$ and or wettability (I_{USBM}).

Numerical database

We used a process based modelling software package (eCore, version 1.3.3., Numerical Rocks, Trondheim, Norway) to generate a suite of rock models. This package makes it possible to simulate the end result of the geological process that forms the rock, based on a grain size distribution, diagenetic parameters (clay content, quartz cementation) and compaction (Bakke and Øren, 1997). The models were based on predefined grain size distributions for Bentheimer, Fontainebleau, Berea outcrops and one for a reservoir rock.

Porosity and permeability of the models were arbitrarily changed by adjusting the amount of quartz cementation, and by changing the clay content between 1 and 10% (volume %) and/or clay distribution. In total 30 different rock models were made, see Figure 1. The size of the models was 800 cubed with a voxel size between 4-8 μm. The representative elementary volume (REV) for each model was checked using the two-point correlation length (auto-correlation length) (see *e.g.* Keehm and Mukerji (2004)). The model size was at least 20 times the auto correlation length. The simulated k,φ-relationship lies above the experimental relationship. It was not possible to reduce the permeability of the simulated sandstones significantly using the given grain size distributions. To be able to draw a fair comparison, a subset of the experimental data that corresponds to the simulated data is indicated in green (Figure 1, right).

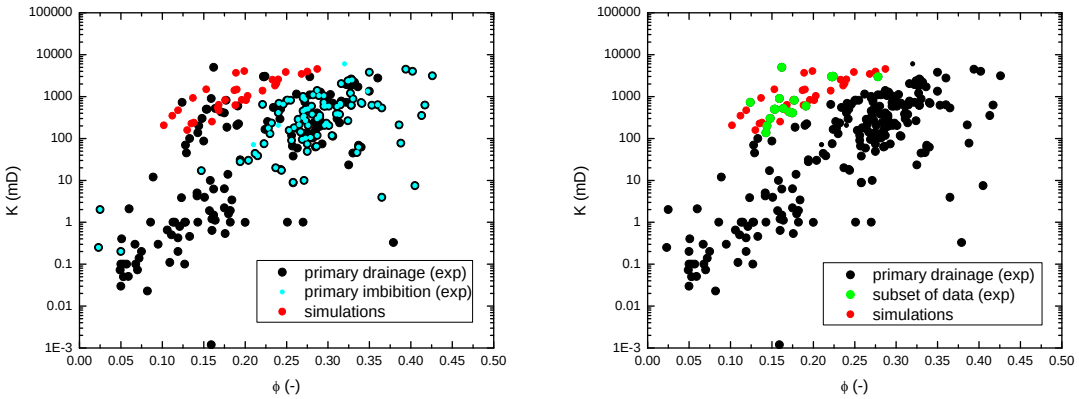

Figure 1 Left: Porosity permeability relationship for the experimental data set compared with the simulated dataset. Right: subset of (primary drainage) experimental data indicated in green.

Subsequently, multi-phase flow simulations on the respective pore network models were performed using eCore's pore network simulator (Bakke and Øren, 1997). For drainage, the contact angle between oil and brine was between 0° and 30°. For imbibition, different scenarios were run, ranging from completely water wet representations to completely oil wet representations. The wettability is factored in by specifying the contact angles between oil and brine for the oil wet and the water wet pores. Three wettability conditions were implemented in the models, see Table 1. In addition, the fraction of pores that changed wettability after drainage is set via the 'oil wet pore fraction', which is a number that can be varied between 0 (completely water wet) to 1 (completely oil wet). The distribution of oil wet pores can be set to 'random', to 'large' pores and to 'small' pores. Simulations were performed with varying contact angles (conditions 1,2 or 3), with varying oil wet pore fractions (between 0 and 1, with increments of 0.1) and with different distributions (small, large, or random). In total, over 2600 simulations were performed.

As a next step, the simulated capillary pressure and relative permeability results were fitted with the aid of the parameterized functions (Eq. (1) – (4)). Wettability indices were calculated from the complete (imbibition and secondary) capillary pressure curves and from the points of spontaneous imbibition. The end point saturations in the simulator are governed by the maximum curvature (maximum capillary pressure) in the system, which is governed by the minimum pore throat size.

Table 1 Wettability conditions for pore network models

Condition	Water wet contact angle distribution (º)	Oil wet contact angle distribution (º)
1	30-60	100-150
2	60-75	105-120
3	30-75	105-180

RESULTS

Primary drainage capillary pressure

Comparisons between the experimental data set and the numerical simulations for the entry pressure P_e on the one hand and for the irreducible water saturation S_{ir} on the other are given in Figure 2. The results for the curve shape factor a are given in Figure 3. The three parameters correlated best with $X=\sqrt{\frac{k}{\varphi}}$, compared to k or φ alone. Correlations were established using a Levenberg-Marquardt fitting algorithm. Error bars of the fit were obtained by taking the standard deviations of binned data points and are shown as thin solid lines. The larger the error bar of an averaged bin, the lower its weight to the fit.

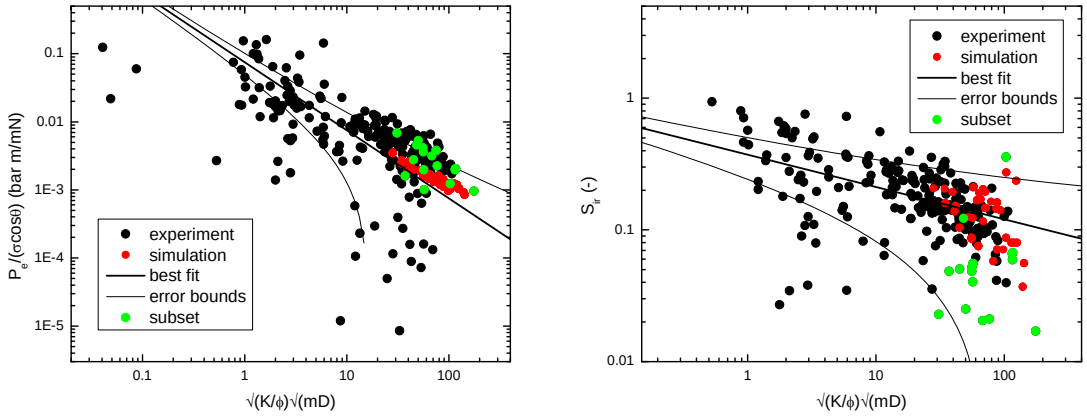

Figure 2 Left: capillary entry pressure P_e as function of √(k/φ). Right: irreducible water saturation, S_{ir}, as a function of the pore geometry factor X.

The comparisons show that the correlations for the entry pressure and the irreducible water saturation fall within the error bars of the experimental data set. The curve shape factor a is low, but compared to the subset of experimental data, the agreement is quite well.

First imbibition capillary pressure curve

The first imbibition capillary pressure curve is affected by wettability. In Figure 3, experimental data and simulated data is presented in terms of Amott-Harvey and USBM wettability indices. To be able to make a fair comparison between experiment and simulation, a subset of simulated data having similar wettability as the experimental data (on the basis of Amott-Harvey index: $-0.3 < I_{AH} < 0.5$) is indicated in the subsequent plots.

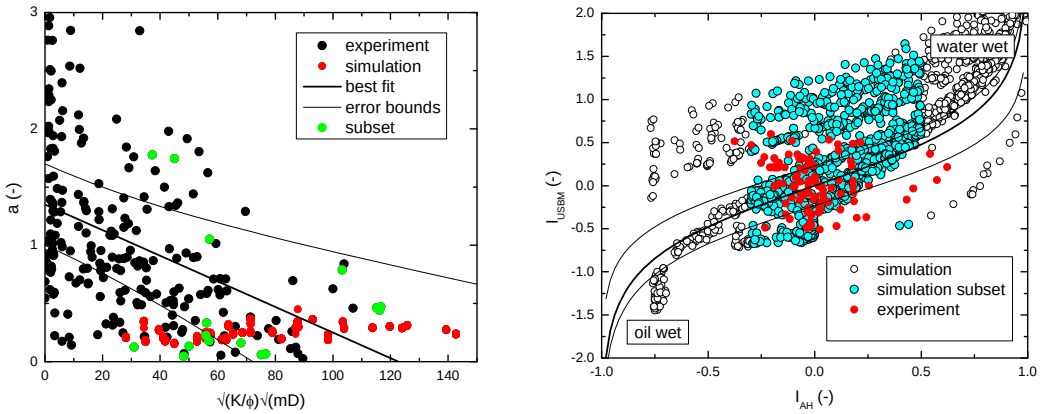

Figure 3 Left: curve shape factor, *a*, as function of the pore geometry factor. Right: Amott-Harvey wettability index vs. USBM wettability index. Solid lines indicate theoretical boundaries for mixed wet large, fractionally wet and mixed wet small cases (v=2, r_{min} = 0.2 µm, r_{max} = 200 µm).

The first imbibition capillary pressure curve can be described by means of the parameters S_{ir}, S_{or}, c_w, c_o, a_o and a_w, see Eq. (2). The irreducible water saturation does not change during the imbibition process, hence it is similar as what was found for primary drainage. The parameters c_o and c_w are related to the entry pressures for the oil wet pores and water wet pores respectively. For a completely oil wet rock, the entry pressure for the water should equal the entry pressure for the oil during drainage (Masalmeh and Jing, 2006). In that (hypothetical) case, the same relationship between c_o and X should be expected as between P_e and X for drainage. By normalizing the c_o factor with this relationship, one would expect to find its dependency on wettability. In Figure 4 we have plotted c_o, normalized with the interfacial tension and with (0.075/X). The latter represents the solid line in Figure 2. The wettability index I_{USBM} was converted, so that is between 0 (water wet) and 1 (oil wet) by using

$$W_{USBM} = 0.5 \cdot \left(1 - \frac{\arctan(I_{USBM})}{\pi/2}\right), \tag{5}$$

where W_{USBM} is the new wettability index. The simulated values for c_o are on average higher than the experimental ones, also those from the subset. Simulated values for c_w are also higher than the experimental data. The latter can be explained by the fact that the experimental imbibition curves are not very reliable at low saturations, and it was found that most experimental curves could be fitted nicely using zero for c_w.

The residual oil saturation is plotted as the *mobile oil saturation* versus the *initial oil saturation* in Figure 5. For the experimental data, an almost linear trend is visible. The simulated data (also the subset) is much more widely scattered around the linear trend. Close inspection of the data shows that the higher points are associated with oil wet rocks, whereas the lower points are associated with very water wet rocks. It is well known that in oil wet rocks, oil can flow via films to very low residual values, hence S_{or} = 0. In that case, the initial oil saturation equals the mobile oil saturation. For the

experiments, however, no clear correlation between S_{or} and X or wettability was found (figures not shown).

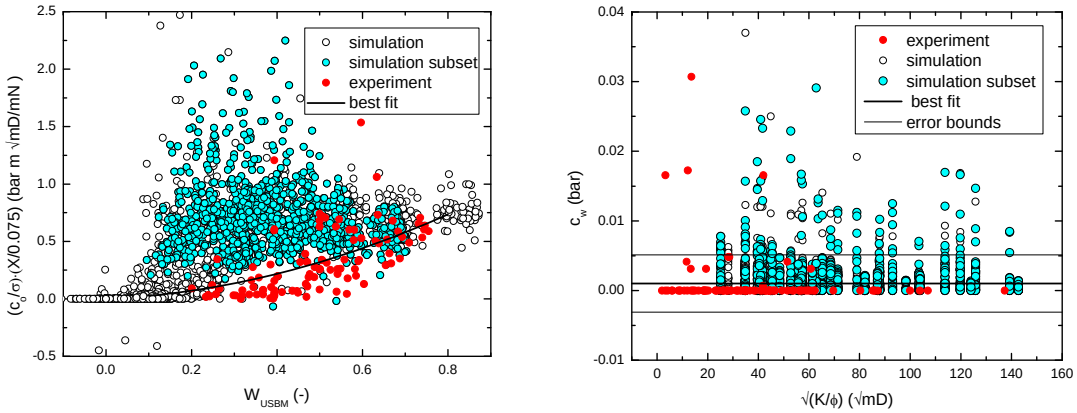

Figure 4 Left: Oil entry pressure, c_o normalized with the pore geometry factor X and interfacial tension σ, as a function of the wettability W_{USBM}. Right: water 'entry pressure' for imbibition, c_w, as a function of the pore geometry factor.

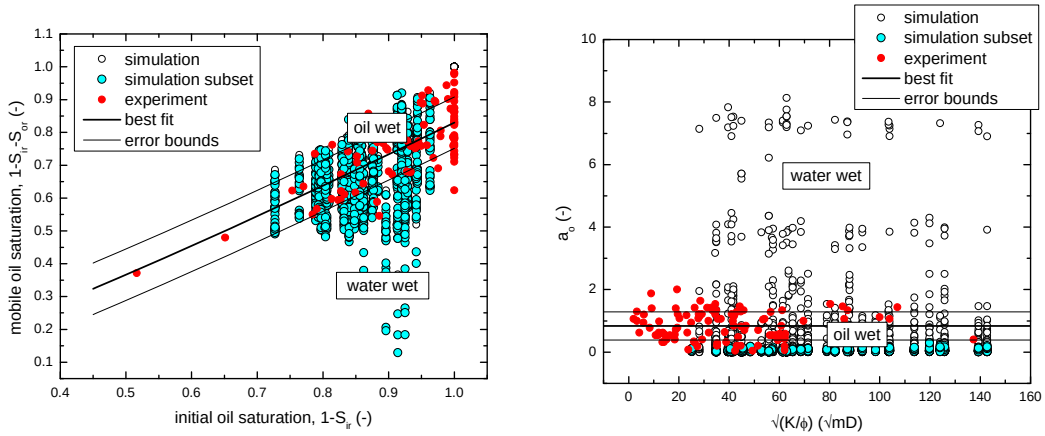

Figure 5 Left: mobile oil saturation as a function of initial oil saturation. Right: oil curve shape factor for imbibition as a function of the pore geometry factor.

The curve shape factor a_w is associated with the curvature of the imbibition curve at low water saturations; the factor a_o is linked to the curvature at higher water saturations. The scatter in simulated a_o is quite large, ranging from 0 to 8, see Figure 5. It was found that for the simulations, the oil wet cases are grouped along the line $a_o = 0.1$. Higher values for a_o relate to more water wet rocks. Simulated results fall in the more oil wet range.

The parameter a_w was fixed at 0.2 for most of the experimental curve fits, for the same reason as was mentioned before: the part at low water saturation is not very reliable from an experimental point of view. The simulated results also include the positive part of the imbibition capillary pressure curve, making it possible to fit the whole curve and obtain

an meaningful value for a_w, see Figure 6. Note that in combination with $c_w = 0$, any value for a_w would give a good fit with the experimental data since the first term drops out of Eq. (2).

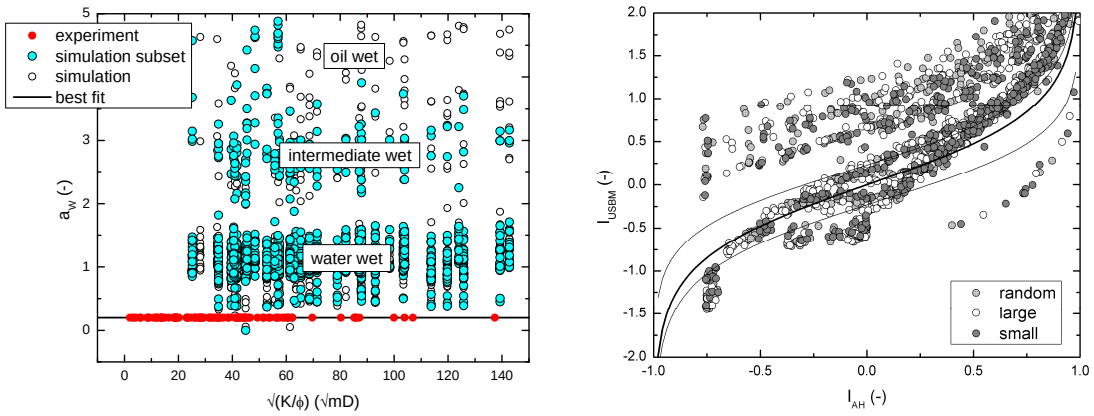

Figure 6 Left: water curve shape factor for imbibition as a function of pore geometry factor. Right: Amott-Harvey wettability index vs. USBM wettability index for numerical simulations on pore network models with different assigned wettability distributions: random, large and small. Solid lines indicate theoretical boundaries for mixed wet large, fractionally wet and mixed wet small cases (v=2, r_{min} = 0.2 µm, r_{max} = 200 µm).

Wettability

For the experimental data, the USBM wettability index was calculated – according to the standard (Donaldson *et al.* (1969)) – from the areas under the first imbibition and secondary drainage capillary pressure curve vs. *average* saturation. The USBM index for the simulations. however, was calculated from the actual capillary pressure curves. The Amott-Harvey wettability index was calculated from the points of spontaneous imbibition (Amott, 1958). Dixit *et al.* (2000) introduced a theoretical framework where points in the I_{USBM}-I_{AH} diagram can be grouped into different classes: mixed wet small, mixed wet large and fractionally wet. According to the theory and supporting pore network simulations, fractionally wet data points should fall on or near the solid thick line in Figure 3. Mixed wet large rocks should be above the upper thin solid line and mixed wet small rocks should be below the lower thin solid line.

The eCore software allows us to run simulations with different fractions of oil wet pores, where the distribution of oil wet pores can be selected to preferentially small pores, preferentially large pores or random. This should correspond to mixed wet small, mixed wet large and fractionally wet. In Figure 6, data points from the three wettability classes are shown, as well as the theoretical boundaries according to Dixit *et al.* (1998). Some experimental confirmation of the existence of wettability classes was found by Skauge *et al.* (2007). They used USBM and Amott-Harvey wettability indices in combination with environmental SEM results. The present study, however, shows that the results from the three wettability classes do not group according to the theory: data points from the three wettability classes are scattered over the diagram and do not fall into the zones indicated

by the trend lines. Most of the data would be classified as fractionally wet or mixed wet large, in contrast to the actual wetting state of the models. Moreover, no correlation with the wettability classes 1,2 or 3 (Table 1) was found and also, no correlation between wettability class and rock type was found (figure not shown).

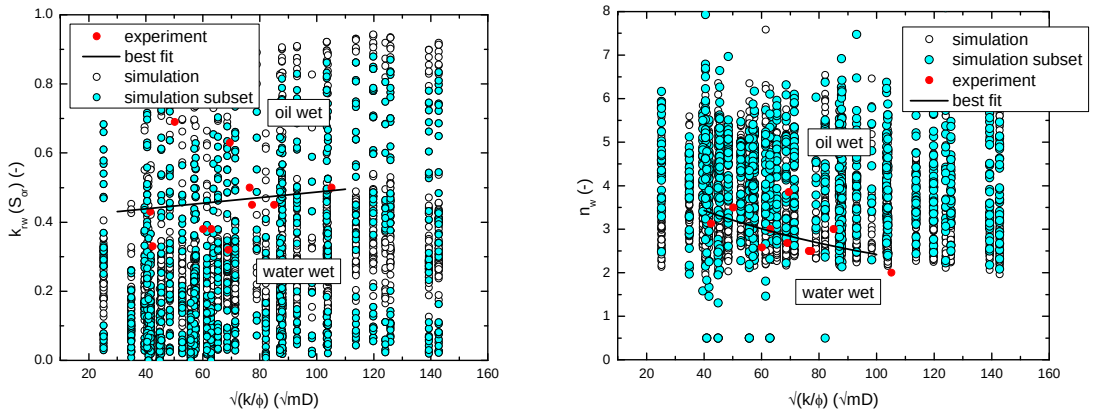

Figure 7 Left: end point water relative permeability as a a function of pore geometry factor. Right: water Corey exponent as a function of pore geometry factor.

First imbibition relative permeability

Relative permeabilities were normalized against the end point oil relative permeability at connate water saturation, so that $k_{ro}(S_{ir})$ equals 1 by definition. Simulated relative permeabilities were normalized in the same manner. In Figure 7, the experimental end point water relative permeabilities are compared against the results from simulations. Note that the experimental data from 74 core samples was averaged for each of the 10 reservoirs, hence only 10 data points are shown. The average simulated $k_{rw}(S_{or})$ is lower than the experimental average. Compared with the simulations, all experimental core plugs should be considered intermediate wet ($I_{AH} \approx 0$). The water Corey exponents are shown in Figure 7, and oil Corey exponents are shown in Figure 8. Based on n_w the experiments should be considered water wet ($I_{AH} \approx 0.8$), and based on simulated results for n_o, we should consider the experimental data oil wet. This gives an inconsistent picture. Simulated values for n_o are lower than the average experimental values.

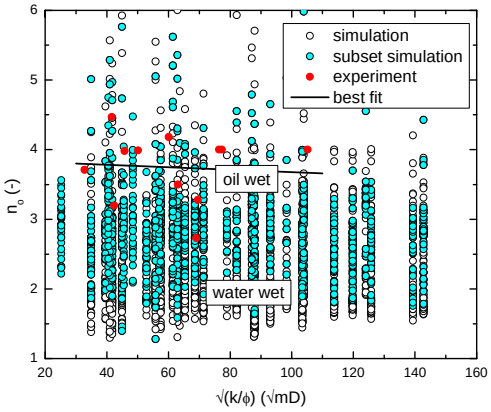

Figure 8 Oil Corey exponent as a function of pore geometry factor.

CONCLUSION

We compared an experimental dataset with a simulated dataset by comparing the parameters that describe the primary drainage and primary imbibition capillary pressure curves and the imbibition relative permeability curve. It was found that the (primary drainage) capillary entry pressure, P_e, the irreducible water saturation, S_{ir}, and the curve shape factor a from the simulations (having a similar porosity-permeability relationship) fall within the error bar of the subset of the experimental data set.

The simulations for imbibition capillary pressure do not agree well with the experimental data. The lack of agreement can be attributed to systematic experimental errors, to curve fitting errors such as non-unique solutions, or to assumptions made in the numerical simulator .

Wettability of the pore networks was altered by 1) changing the range of contact angles of the water wet and oil wet pores, 2) changing the fraction of oil wet pores, 3) changing the distribution of the oil wet pores. It was found that none of the imbibition capillary pressure or relative permeability parameters correlated with the first parameter. Logically, the rocks were made more oil wet by increasing the fraction of oil wet pores. Changing the distribution of oil wet pores (small, large or random) in the simulations did not show a similar trend in the I_{AH}, I_{USBM} diagram as was found by Dixit *et al.* (1998).

Imbibition relative permeability simulations show an inconsistent trend with the experimental data. By comparing experimental values for $k_{rw}(S_{or})$ with simulations, our rocks should be classified as intermediate wet. Based on values for n_w they should be water wet and based on values for n_o the rocks should be oil wet. The simulations suggest that high values for n_w correspond to oil wet rocks and that low values correspond to water wet rocks. According to our experimental data, this relationship should be *vice versa*, and this observation was also found by Stiles (2007).

The current study shows that differences exist between experimental and simulated multi-phase flow properties. This could be due to systematic errors in the experimental data set, but it may also indicate weaknesses of the physical assumptions which are made in the pore network modelling process. More work is needed to fine tune the simulated data set to the experimental data set to generalize the conclusions.

REFERENCES

1. Amott, E. (1959) Observations relating to the wettability of porous rock. *Petroleum Transactions, AIME*. **216**, 156-162. SPE1167-G.
2. Bakke, S. and Øren, P.E. (1997) 3-D pore-scale modelling of sandstones and flow simulations in the pore networks. *SPE Journal* **2**, 136-149. SPE35479.
3. Brooks, R. and Corey, A. (1964). Hydraulic properties of porous media. *Hydrology* Papers, (3).
4. Caubit, C., Hamon, G., Sheppard, A.P., Øren, P.E. (2008) Evaluation of the reliability of prediction of petrophysical data through imagery and pore network modelling. *Proceedings of the International Symposium of the Society of Core Analysts*. SCA2008-33.
5. Dixit, A.B., Buckley, J.S., McDougall, S.R. and Sorbie, K.S. (1998) Core Wettability: Should IAH equal IUSBM? *Proceedings of International Symposium of the Society of Core Analysts*, SCA-9809.
6. Dixit, A.B., Buckley, J.S., McDougall, S.R. and Sorbie, K.S. (2000) Empirical measures of wettability in porous media and the relationship between them derived from pore-scale modelling. *Transport in Porous Media*. **40**, 27-54.
7. Donaldson, E.C., Thomas, R.D., Lorenz, P.B. (1969). Wettability determination and its effect on recovery efficiency, *SPE Journal*, **9**, 13-20. SPE2338
8. Fatt, I. (1956) The network model of porous media I. Capillary pressure characteristics. *Transactions of the American Institute of Mining A*, **207**, 144-159.
9. Keehm, Y. and Mukerji, T. (2004). Permeability and relative permeability from digital rocks: Issues on grid resolution and representative elementary volume. *SEG Int'l Exposition and 74th Annual Meeting, Denver, Colorado*.
10. Masalmeh, S.K. and Jing, X.D. (2006). Capillary pressure characteristics of carbonate reservoirs: relationship between drainage and imbibition curves. *Proceedings of the International Symposium of the Society of Core Analysts*, SCA2006-16.
11. Øren, P.E., Bakke, S., Arntzen, O.J. (1997) Extending predictive capabilities to network models. *SPE Journal*, **3**, 324-336. SPE38880
12. Øren, P.E., Bakke, S., Rueslåtten, H.G. (2006) Digital core laboratory: rock and flow properties derived from computer generated rocks. *Proceedings of International Symposium of the Society of Core Analysts*. SCA2006-21.
13. Quiblier, J. A. (1984) A new three-dimensional modelling technique for studying porous media, *Journal of Colloid Interface Science* **98**, 84–102.
14. Sakellariou, A., Sawkins, T.J., Senden, T.J. and Limaye, A. (2004) X-ray tomography fro mesoscale physics applications. *Physica A* 339, 152-158.

15. Skauge, A., Spildo, K., Høiland, L. and Vik, B. (2007). Theoretical and experimental evidence of different wettability classes. *Journal of Petroleum Science and Engineering*. 57, 312 – 333.
16. Skjaeveland, S., Siqveland, L, Kjosavik, A., Hammersvold Thomas, W., and Virnovsky, G. (2000). Capillary pressure correlation for mixed-wet reservoirs. *SPE Reservoir Evaluation & Engineering*, **3**, 60-67. SPE39497
17. Stiles, J. (2007) Using special core analysis in reservoir engineering. *Imperial College course notes*.
18. Suicmez, V.S., Touati, M. (2007) Pore network modelling: a new technology for SCAL predictions and interpretations. *SPE Saudi Arabia Section Technical Symposium.* SPE110961.
19. Valvatne, P.H., Blunt, M.J. (2003) Predictive pore-scale network modeling. *SPE Annual Technical Conference and Exhibition.* SPE84550